We are IntechOpen,
the world's leading publisher of
Open Access books
Built by scientists, for scientists

6,900
Open access books available

185,000
International authors and editors

200M
Downloads

154
Countries delivered to

Our authors are among the

TOP 1%
most cited scientists

12.2%
Contributors from top 500 universities

CLARIVATE ANALYTICS
BOOK CITATION INDEX
INDEXED

WEB OF SCIENCE™

Selection of our books indexed in the Book Citation Index
in Web of Science™ Core Collection (BKCI)

Interested in publishing with us?
Contact book.department@intechopen.com

Numbers displayed above are based on latest data collected.
For more information visit www.intechopen.com

Synthesis of Two-Frequency Symmetrical Radiation and Its Application in Fiber Optical Structures Monitoring

Oleg Morozov, German Il'in, Gennady Morozov and Tagir Sadeev
Tupolev Kazan National Research Technical University,
Institute of Radio Electronics and Telecommunications
Russia

1. Introduction

Photonics plays the leading role in the decision of some major social, scientific and technical problems, such as, development, exploitation safety and QoS increasing of telecom lines. Efficiency of photometric methods is defined, first of all, by high informative effects of direct interaction of optical radiation with optical fiber.

Method of optical reflectometry (MOR), as one of the most effective photometric methods, is the powerful tool for creation of optical fiber structures monitoring systems (Barnoski & Jensen, 1976). The present stage of reflectometric systems development is directed on the further improvement of their characteristics, research of new principles of probing and registration of backscattering information, development of precision measuring converters and is based on use of systems with continuous wave radiation. Such accent is explained, firstly, by power equivalence of pulse probing with high peak power and small duration of a pulse and continuous probing with low power of radiation and big time of supervision, secondly, by the fulfilled technique of spatially - resolved measurements based on the linear frequency modulation method, and thirdly, by the significant progress in the field of creation of hi-tech and inexpensive element base (sources of radiation with the big coherence length, broadband devices of radiation parameters control and high-speed photoreception devices).

Overwhelming majority of open and built-in continuous wave reflectometric systems represent homodyne systems in which carrying frequencies of referent and measuring channels coincide. Such systems possess a simple design and an opportunity of direct allocation and registration of information signal. However during photo-electric transformation the low-frequency noise characteristic of structural units, noise characteristics of radiation sources and photo detectors play essential role that considerably worsens metrological characteristics, and also functionalities of the specified systems. The decision of homodyne reflectometric system problems is based on the use of two-frequency methods. In this case, systems will be transformed in heterodyne type where frequencies of basic and measuring channels do not coincide, and displacement of frequencies is achieved due to use of devices forming two-frequency laser radiation.

We have proposed and demonstrated in recent years an unique technique to synthesize the two-frequency radiation by manipulating the amplitude and the phase of initial one frequency lightwave (Il'in & O.G. Morozov, 1983, Il'in et al., 1996, O.G. Morozov & Pol'ski, 1996). The output frequencies are symmetrical relatively to suppressed initial one and have equal amplitudes and alternative phases.

We consider the set of the analysis and synthesis problems which should be solved by development of the theory and technical equipment of optical reflectometers for fiber optical structures (FOS) monitoring in optical two-frequency domain (OTFDR) (Pol'ski & O.G. Morozov, 1996, 1998, Zalyalov et al., 1998, O.G. Morozov et al., 1999). Based upon this technique, the synthesis of two-frequency symmetrical probing radiation (TFSPR), various photonic sensing of fiber optic structures and optical information-processing applications have been developed (Natanson et al., 2005a, 2005b, O.G. Morozov et al., 2006, O.G. Morozov & Aybatov, 2007, O.G. Morozov et al., 2008a, O.G. Morozov et al., 2010).

In this chapter, the principle of TFSPR synthesis is summarized. A series of functional optical-sensing OTFDR systems, including fiber-optic reflectometres, multiplexed fiber Bragg grating (FBG) or fiber Fabry-Perault interferometers (FFPI) sensors are introduced. Fully distributed fiber-optic strain sensing system based on Brillouin frequency shift is highlighted (Natanson et al., 2005a, G.A. Morozov et al., 2011), and four wave mixing compensating system (O.G. Morozov et al., 2008b) based on optimized TFSPR is also presented. Miscellaneous OTFDR applications in biosensors (O.A. Stepustchenko et al., 2011) and two-frequency signal forming for photonic microwave filters synthesis (O.G. Morozov et al., 2009, O.G. Morozov & Sadeev, 2011) are also reviewed.

2. Synthesis of two-frequency symmetrical probing radiation

Theoretical motivation of original method of one-frequency radiation transformation into two-frequency ones (named as Il'in-Morozov method) is considered in this part (Il'in & O.G. Morozov, 1983).

Realization of this method allows getting an output two-frequency oscillation with high degree of spectrum purity. Herewith, there are ensured high transformation factor and stability of output spectrum parameters at the deflection of transformation parameters from optimum, as well as possibility of differential frequency tuning on the given law and with the given velocity.

2.1 Theoretical basis

Initial single-frequency oscillation (fig. 1) is described as

$$e(t) = E_0 \sin \varphi(t) , \qquad (1)$$

where $\varphi(t) = \omega_0 t + \varphi_0$ is phase change, and E_0, ω_0, φ_0 are its permanent amplitude, frequency, and initial phase correspondingly.

From theory of modulated signals it's known that phase modulation with certain indexes could decrease (eliminate) amplitude of initial (carrier) frequency and produce two symmetric side lobes (Kharckevich, 1962). Let's consider an oscillation with following $\varphi(t)$ commutation

$$e(t) = E_0 \begin{cases} \sin\omega_0 t & \text{when} \quad T(2p-1)/2 < t \le Tp \\ \sin(\omega_0 t + \theta) & \text{when} \quad Tp < t \le T(2p+1)/2 \end{cases}, \tag{2}$$

where $T = 2\pi/\Omega$, $\Omega = \omega_0/k$, θ are period, frequency, and phase change, correspondingly, $k \gg 1$ is integer, and $p = 0, 1, 2,...$ When $\theta = \pi$ Fourier expansion of equation (2) is given by

$$e(t) = \frac{2E_0}{\pi} \sum_n \frac{1}{n} \{\cos(\omega_0 + n\Omega)t - \cos(\omega_0 - n\Omega)t\}, \tag{3}$$

where $n = 1, 3, 5$ is harmonic number of phase change frequency expansion.
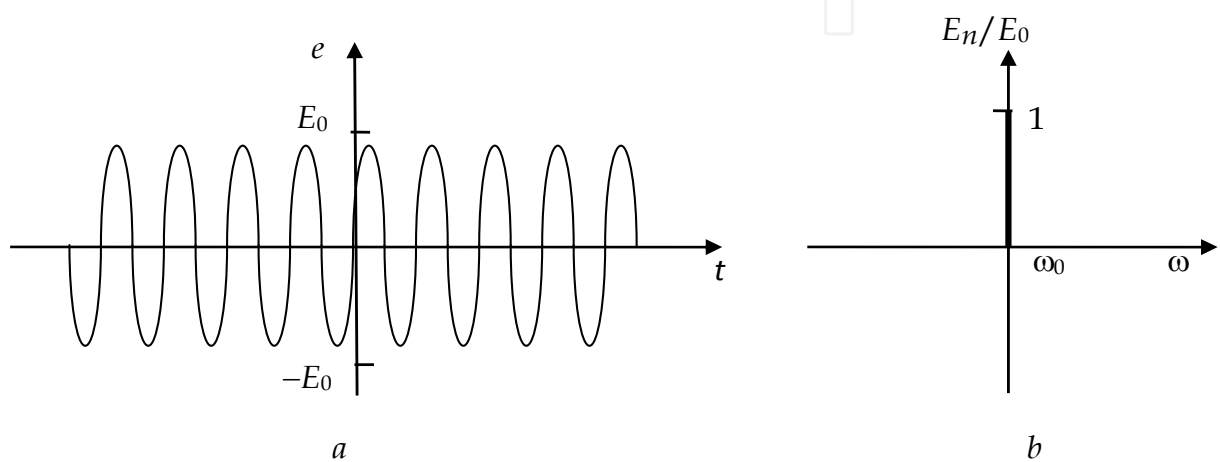
Fig. 1. Timing chart (*a*) and spectrum of Fourier series coefficients (*b*) of (1)

Thus, oscillation (2) is two-band multi frequency oscillation with intercarrier frequency between spectral components equals 2Ω, and suppressed carrier (fig. 2). Initial phases of spectral components inside bands are equal, and difference between initial phases of lower and upper bands is π.
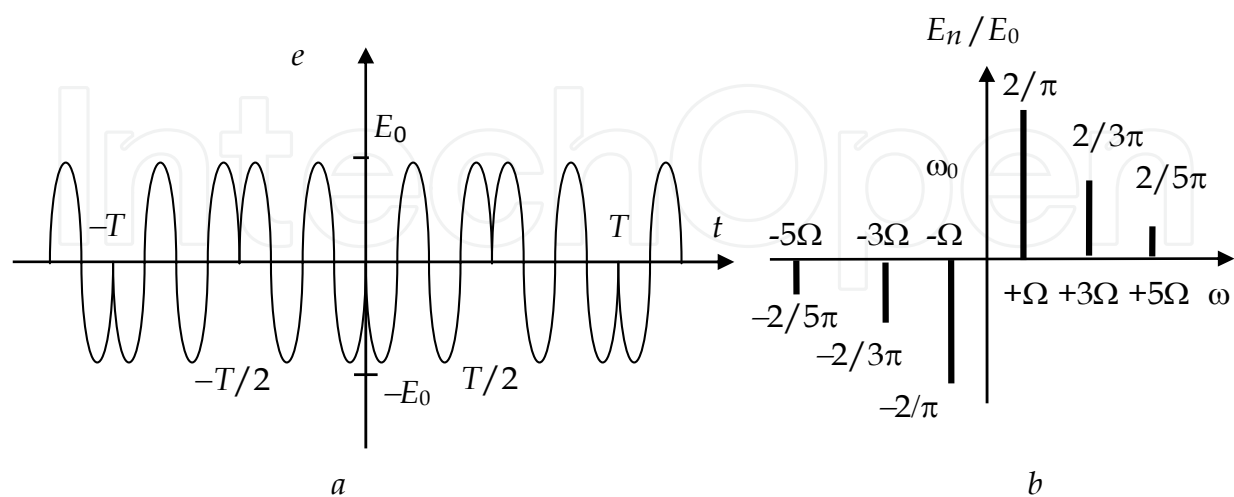

Fig. 2. Timing chart (*a*) and spectrum of Fourier series coefficients (*b*) of (2)

The task of following investigation consists in searching methods of forming two-frequency oscillation from two-band oscillation (3).

2.2 Methods of two-frequency oscillation forming

According to the theory of modulated signals (Kharckevich, 1962) and analysis of spectrum characteristics (3) we can suppose that suppression of its spurious products for forming two frequency oscillation is possible after amplitude modulation of oscillation (2) by some signal S(t), which satisfies the following demands.

During amplitude modulation of single-frequency oscillation by S(t) is produced amplitude modulated signal with frequency spacing between carrier and the nearest side components and between side components at each band equals 2Ω. The difference between carrier initial phase and side band components initial phase is π. Initial phases of side components inside bands are equal.

The simplest oscillation, which satisfy that demands, is $S_1(t) = S_1 \cos(2\Omega t + \pi)$, where S_1 is its permanent amplitude, π is initial phase. In case of oscillation (2) amplitude modulation by signal $S_1(t)$, we will get the resulting oscillation (fig. 3)with the following spectrum

$$e(t) = \frac{2E_0}{\pi} \sum_n \left\{ \left[\frac{1}{n} - \frac{m}{2} \left(\frac{1}{n-2} + \frac{1}{n+2} \right) \right] \left[\cos(\omega_0 + n\Omega) t - \cos(\omega_0 - n\Omega) t \right] \right\}, \tag{4}$$
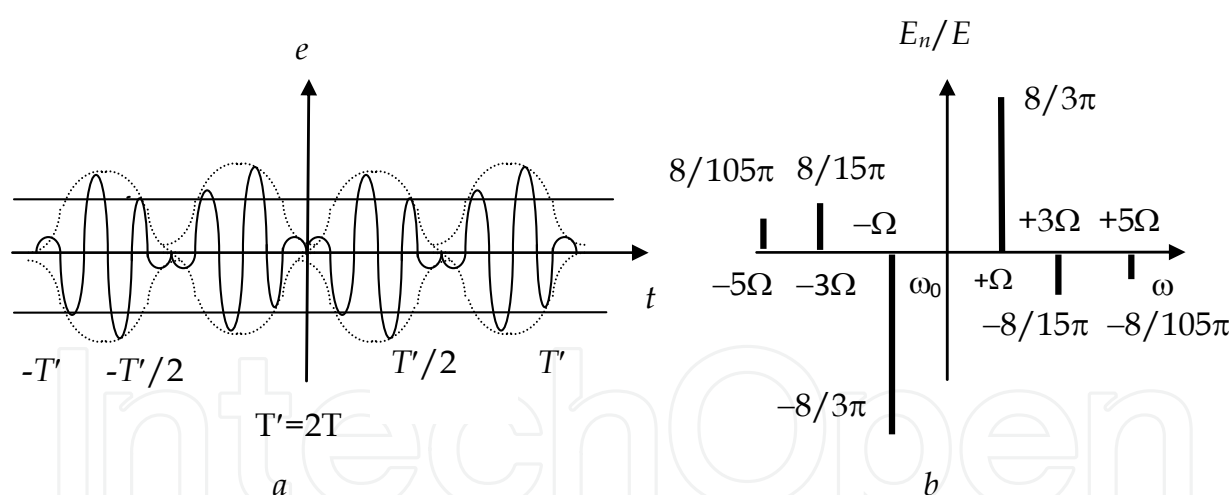
where *m* is the amplitude modulation index.

Fig. 3. Timing chart (*a*) and spectrum of Fourier series coefficients (*b*) of (4)

From (4) follows that the first item in square brackets defines spectrum of Fourier series indexes (3), and the second and the third items describes suppression influence at its components. The level of suppression depends on modulation index *m*. If we take $E_3 = 0$, we will receive the optimal modulation index $m_{opt} = 5/9$, and the resulting oscillation will be almost two-frequency ($E_1 = 0{,}76E_0$), because the amplitude of spectral components $E_n \le E_1/15$ for $n \ge 5$. Varying the modulation index within $(0{,}85 - 1{,}15)m_{opt}$ the output oscillation nonlinear-distortions coefficient would not exceed one percent.

Total suppression of side components with numbers $n \geq 3$ we could achieve with modulating signal $S_2(t) = S_0|\sin\Omega t|$.

In that case the resulting oscillation will have the following spectrum

$$e(t) = \frac{2E_0}{\pi}(1-b)\sum_n \frac{1}{n}\left[\cos(\omega_0 + n\Omega)t - \cos(\omega_0 - n\Omega)t\right] + \frac{\pi E_0 b}{4}\left[\cos(\omega_0 + \Omega)t - \cos(\omega_0 - \Omega)t\right], \quad (5)$$

where b is amplitude modulation index.

Spectral components amplitudes will be defined by Fourier series indexes and for $n=1$ $E_1=[2E_0/\pi][1-b]+[\pi E_0 b/4]$, for $n \geq 3$ $E_n=[2E_0/\pi n][1-b]$. When $b_{opt}=1$ the spectrum contains two useful components with frequencies $\omega_0+\Omega$ and $\omega_0-\Omega$, and spurious components are suppressed (fig. 4). Varying the modulation index within $(0,7-1)b_{opt}$ the output oscillation nonlinear-distortions coefficient would not exceed one percent.
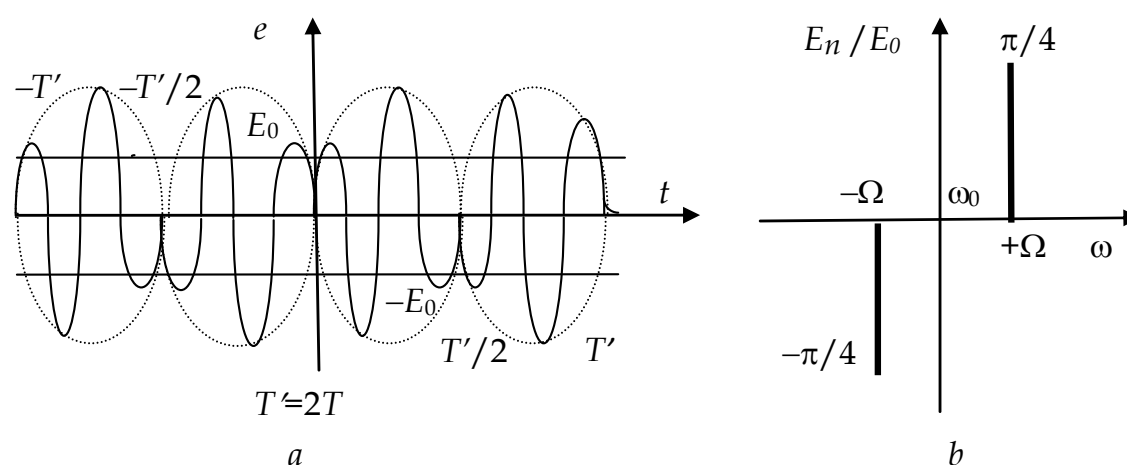

Fig. 4. Timing chart (*a*) and spectrum of Fourier series coefficients (*b*) of (5)

2.3 Discussion of the results

Thus, amplitude-phase method of one-frequency oscillation conversion into two-frequency ones, or Il'in-Morozov method, can be formulated as: conversion of a single-frequency coherent radiation in the two-frequency, based on an external electro-optic modulation, which performs the amplitude modulation of single-frequency coherent radiation by a factor equal to 1 and the phase commutation of the received amplitude modulated radiation at π for each envelope passage through its minimum.

Intercarrier frequency of two-frequency oscillation (5) when $b_{opt}=1$ is defined by frequency Ω of phase commutation θ. Its stability unambiguously concerned with frequency stability of driving voltages and instabilities of commutations devices. Really achievable value of intercarrier frequency's instability with simple thermo stating of driving generators is 10^{-6}. Intercarrier frequency's retuning, which is required in some types of measurements, is rather simple realized with the use of amplitude-phase conversion, minimum frequency shift is determined by modulators gain slope, and maximum frequency shift is determined by higher cutoff frequency of modulator and correlation between modulatory and modulated frequencies.

Energy equality of side lobes and the effectiveness of their conversion are of great importance in multi frequency systems. Using the derived equations for the spectrums of output oscillations and taking into consideration properties of amplitude-phase conversion, i.e. using the additional power of amplitude modulation and phase commutation for forming the side lobes, we could determine, that power of the last one is nearly 60 percent of initial single-frequency oscillation, and conversion index equals unit value without taking into account the loss in real modulators.

3. Information structure of symmetric two-frequency oscillation

Symmetric two-frequency oscillation is complex signal with amplitude and phase modulation. Main feature of this signal is that all its components (envelope $A(t)$, instantaneous phase $\theta(t)$ and frequency $\omega(t)$) are periodic functions with period $T = (1/2\pi)\Omega$ and depend on its components amplitude ratio A_1/A_2. Let's define the parameters, which could be used for registration in measuring system and carry information about interaction between two-frequency oscillation and structure under investigation. As such parameters could be used amplitude modulation factor, gradients of phase and frequency changes.

1. Let's evaluate modulation rate of two-frequency signal. Thereto we will use the modulation coefficient (Gonorovski, 1977) $m = 2(A_{max} - A_{min})/2(A_{max} + A_{min})$. Calculation results of $m(A_1/A_2)$ are shown on fig. 5. Analysis of the dependence $m(A_1/A_2)$ allows determination of components amplitude ratio with high precision during the measurement of modulation index, and effective realization the feedback process by controlling the instantaneous amplitude of two-frequency signal using its components amplitude ratio.
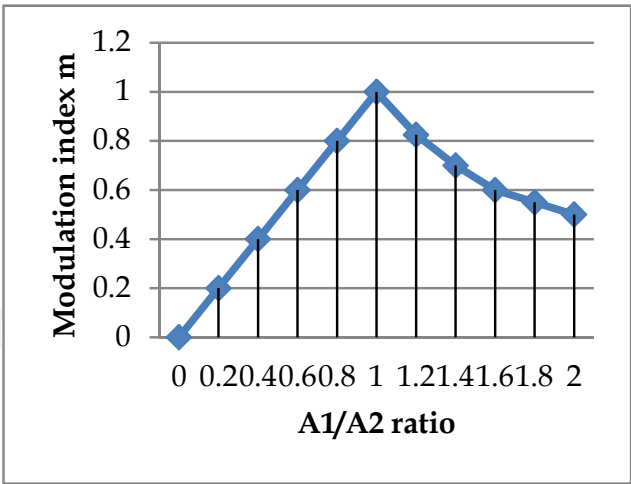

Fig. 5. Dependence $m(A_1/A_2)$

2. Let's define phase gradient of two-frequency signal under its amplitude changing. Calculation results of $\Delta\theta(A_1/A_2)$ are shown at fig. 6. Analysis of the dependence $\Delta\theta(A_1, A_2)$ allows determination of components amplitude ratio with high precision during the measurement of modulation phase, and effective realization the feedback process by controlling the instantaneous phase of two-frequency signal using its components amplitude ratio.
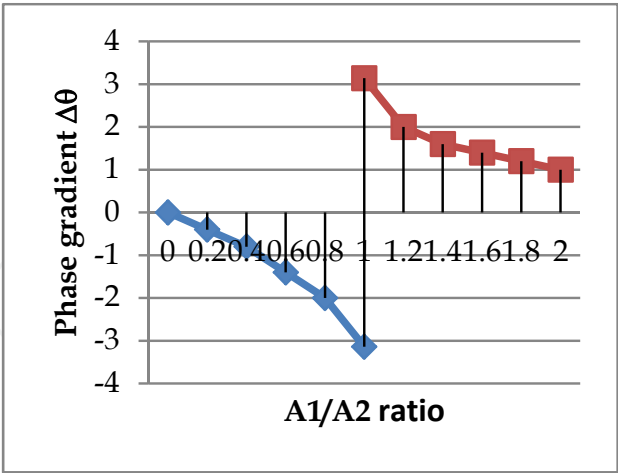
Fig. 6. Dependence $\Delta\theta(A_1/A_2)$

3. Let consider gradient of two-frequency signal instantaneous frequency under its amplitude changing. Calculation results of instantaneous frequency overriding $|\Delta\omega|$ dependence on amplitude components ratio A_1/A_2, $\Delta\omega(A_1, A_2)$ are shown at fig. 7.
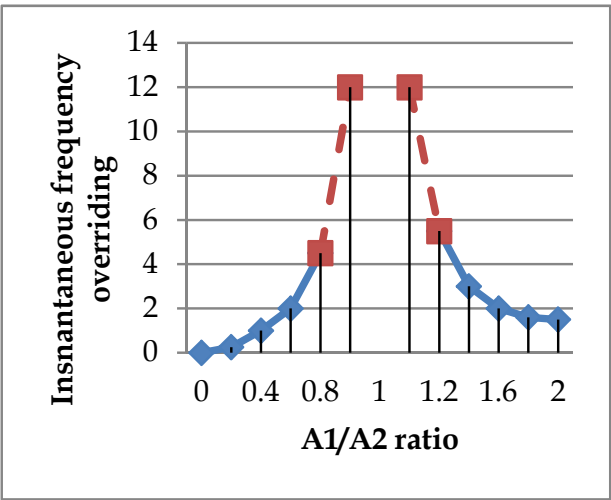

Fig. 7. Dependence $|\Delta\omega|(A_1/A_2)$

Unlike previous cases analysis of the dependence $|\Delta\omega|(A_1/A_2)$ allows determination of components amplitude ratio during the changes of modulation frequency, and effective realization the feedback process by controlling the instantaneous frequency of two frequency signal using its components amplitude ratio in some limits (overriding).

Dependence of instantaneous frequency normalized to frequency distortion $\omega/\Delta\omega$ $(\Delta\omega = \omega_2 - \omega_1)$ on amplitude components ratio A_1/A_2 is more informative. Calculation results of $(\omega/\Delta\omega)$ as function from (A_1/A_2) are shown at fig. 8. Average frequency of two-frequency signal fluctuates with changes of components amplitude ratio in range limited by frequencies of two-frequency signal. When components amplitudes are equal, the average frequency is situated in the middle of that range and has the value $\omega_a = (\omega_1 + \omega_2)/2$.
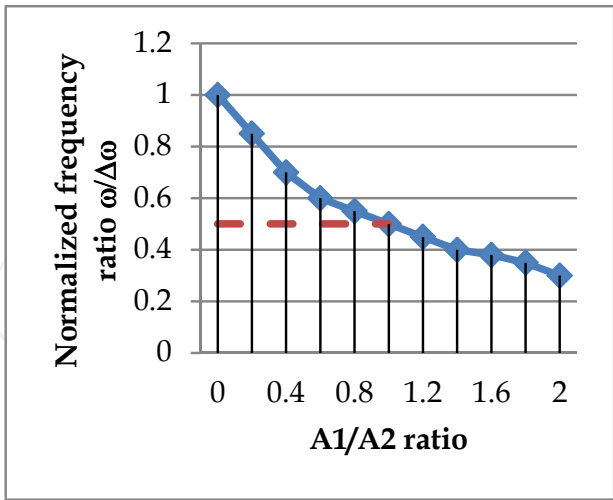
Fig. 8. Dependence $|\omega/\Delta\omega|(A_1/A_2)$

On the basis of two frequencies signal information structure investigation with purpose of finding out main principles of combined interaction of instantaneous values of amplitude, phase and frequency has been defined.

1. Instantaneous phase of two-frequency signal has a sawtooth dependence. Speed of instantaneous phase changes is defined by components amplitude ratio. If $A_1/A_2 = 1$ the maximal speed of phase changing is observed. When two-frequency envelope has its minimum value, instantaneous phase has a shift, which depends on harmonic components amplitude ratio. If the amplitudes of two-frequency signal components are equal, phase shift is equal to π.
2. It has been shown, that instantaneous frequency of two-frequency signal changes with deviation of it components amplitude ratio in range limited by signal frequencies. In case of components amplitude equality, instantaneous frequency coincides with average frequency of two-frequency signal $\omega_a = (\omega_1 + \omega_2)/2$. When the envelope of two-frequency signal has its minimum value, frequency overriding occurs, which depends on harmonic components amplitudes ratio. When amplitudes of two frequency components are equal, value of frequency overriding is infinity.
3. Modulation coefficient has a linear dependence on amplitudes ratio of two-frequency components. When amplitudes of frequency components are equal, modulation coefficient is maximal and equals unit value.

All obtained dependences could be used in symmetric reflectometric systems as informative and directive functions and in order to get information from selective optical fiber structures, like FBG, IFP, embedded multilayer thin film filter and so on.

4. Questions of method realization in optical range

One of the main purposes of our investigations is to determine the most rational methods of two-frequency laser radiation obtaining and devices for their realization in different regions of IR band. Comparative analysis of radiators characteristics was done in order to achieve this purpose. The main parameters for analysis were following: reproduction of waves

length and their difference frequency, difference frequency range, stability and equality of amplitudes on both radiating frequencies, re-tuning possibility of radiating frequencies by desirable law with desirable speed, linearity of drive characteristic, peculiarities of utilizing in FOS monitoring system composition and cost of technical realization. Some results of analysis are presented in table 1.

Two-frequency radiators and their characteristics	Difference frequency range, MHz	difference frequency instability	Equality and stability of amplitude	Possibility of re-tuning	Purity of output spectrum
Diode laser	1000	10^{-2}	–	NSM (*)	+
Two-mode laser	100	10^{-8}	+	NSM	+
Zeeman's laser	$10^{-3}...100$	10^{-9}	+	NSM	+
Acoustooptic	$10^{-2}...100$	10^{-6}	–	+(**)	$\pm$ (***)
Electrooptic:					
polarize	0...20	10^{-6}	–	+	$\pm$ (***)
phase	0...5	10^{-6}	–	+	$\pm$ (***)
amplitude-phase	0...1000	10^{-6}	+	+	$\pm$ (***)

(*) NSM - in these radiators it is necessary to use special means for organizing of re-tuning; (**) + - the organizing of re-tuning is very simple; (***) – it is necessary to use stabilization measures to decrease parasitic components caused by non-stability of modulating parameters and their deviation from optimal.

Table 1. Results of comparative analysis

We can affirm with some care that diode lasers, acoustooptic and electrooptic converters will be widely used. However complexity of control canal realization in first and some uncomfortability of optical schemes in second pull out on first plan the using of electrooptical devices (if the process of their characteristics improvement is rapid and qualitative). It's necessary for this to raise the stability of spectral characteristics and the degree of output radiation spectral purity when the parameters of transformation are deviated from optimal.

So, electro optical devices, possessing the best features for the transformation of coherent radiation parameters, particularly, under the modulating effects, belonging to the microwave range of electromagnetic waves, are choose as the base elements for realization of method in the optical range. Let's examine the problem of output spectrum purity and transformation parameters effect on it, as characteristics which directly determine the accuracy of monitoring on the whole.

Our converter is based on classic amplitude electro-optic modulator on 3m class metaniobat lithium crystal. The output spectrums of converter radiation in different cases are shown on fig. 9. We are the first, who shown (Il'in et al., 1996, 1997), that when converter operated in zero point of modulation characteristic described above Il'in-Morozov method was realized (fig. 9, c) and output spectrum was described as
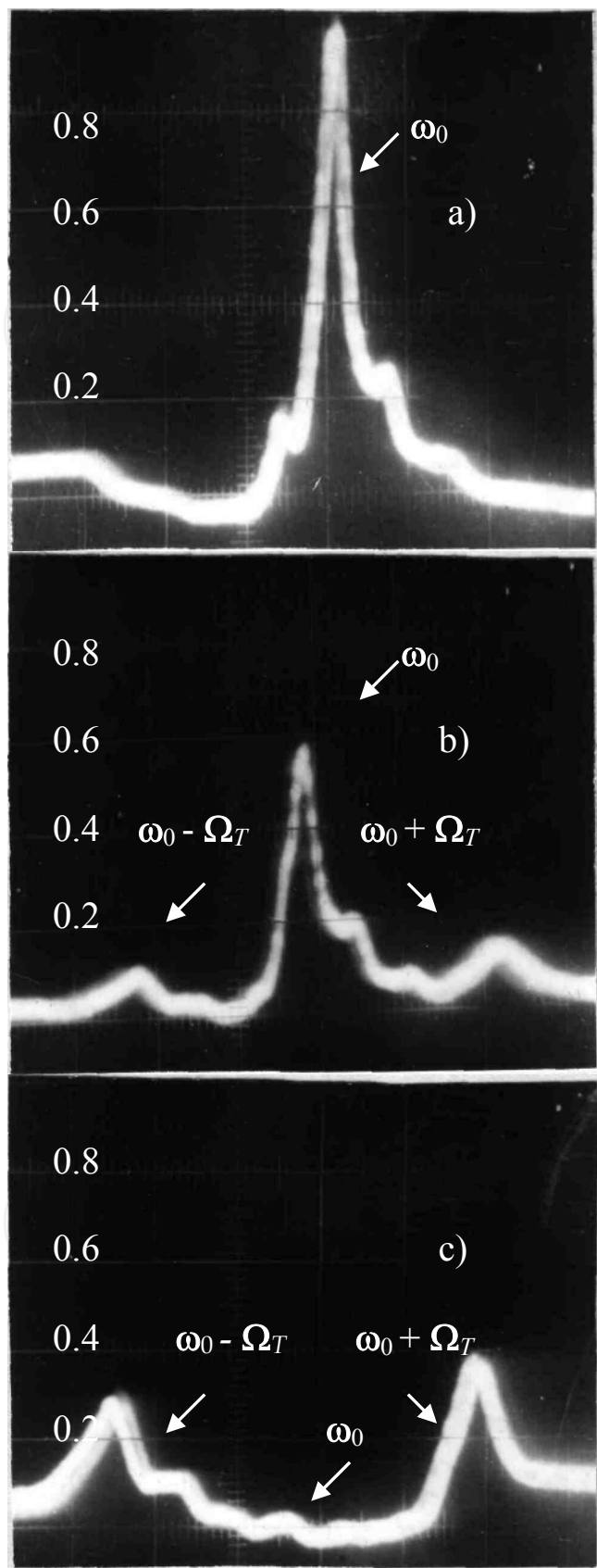
Fig. 9. Output spectrum of amplitude-phase electro optical converter:
a – without modulation; b – amplitude modulation; c – amplitude-phase modulation

$$e(t) = -jE_0 \exp(j\omega_0 t) \times \left[2 \sum_{k=0}^{\infty} J_{2k+1}(z) \sin(2k+1)\Omega_T t \right], \qquad (6)$$

where j is the index, which shows us, that output radiation is orthogonal to initial one; z is parameter, which is determined by the crystal and transforming field characteristics; $J_{2k+1}(z)$ is Bessel's function of (2k+1)-order.

When the value of controlling voltage U_m is equal to half wave voltage $U_{\lambda/2}$ of modulator, then $z = (\pi/2)(U_m/U_{\lambda/2}) = \pi/2$ and $J_1(z)=0{,}64$, $J_3(z)=0{,}06$.

The main causes which make spectral purity worse are temperature non-stability, deviation of transformation parameters from optimal and desalignment of converter. All of them cause the deviation of operating point from zero ($z \neq \pi/2$) and fast growth of parasitic spectral components amplitudes

$$e(t) = -j\frac{\sqrt{2}}{2}\exp(j\omega_0 t) \times$$
$$\times \left[\begin{array}{c} \sum_{k=0}^{\infty} J_0(z) + \\ +2\sum_{k=0}^{\infty} J_{2k+1}(z)\sin(2k+1)\Omega_T t + \\ +2\sum_{k=1}^{\infty} J_{2k}(z)\cos 2k\Omega_T t \end{array} \right]. \qquad (7)$$

Simple special countermeasures, using in converter, make their effect on spectrum purity very inappreciable. The maximum transformation coefficient for (6) is equal to 0,64, but when we choose transformation coefficient equal to 0,58 the coefficient of nonlinear distortions is not exceed 1%. Two more important things we must underline are equality of amplitudes of both spectrum components without dependence from location of working point and simplicity of frequency retuning, which is explained by using of one modulating signal.

Great results are obtained in electro optical integral Mach-Zehnder modulators (MZM) which are broadband, have dimensions 40-60 micrometers with an output of 20-40 mW when integrated micro-and nanotechnologies are used. In most papers devoted to the synthesis of two-frequency MZM formers, the modulation curve of MZM is generally considered in intensity domain as shown in Fig. 10,a. In these circumstances the phase is not taken into consideration and may be determined indirectly.

Consider the spectrum of the MZM output signal for different positions of the bias point on modulation characteristic with respect to the electric field E, as shown in Fig. 10,b. The modulation characteristic of electric field has four distinct regions. We consider the spectrum of the output oscillations under constant bias on behalf of two-frequency former.

The most specific is null bias point. This regime corresponds to the minimum output voltage $\Phi_{bias}=\pi$. The output signal is described by (8-9), where E_0, ω – amplitude and angular frequency of the electric field input CW optical signal; b – modulation index; Ω, V_{mod} – angular frequency and amplitude of modulating signal; V_π - half-wave voltage of the modulator.
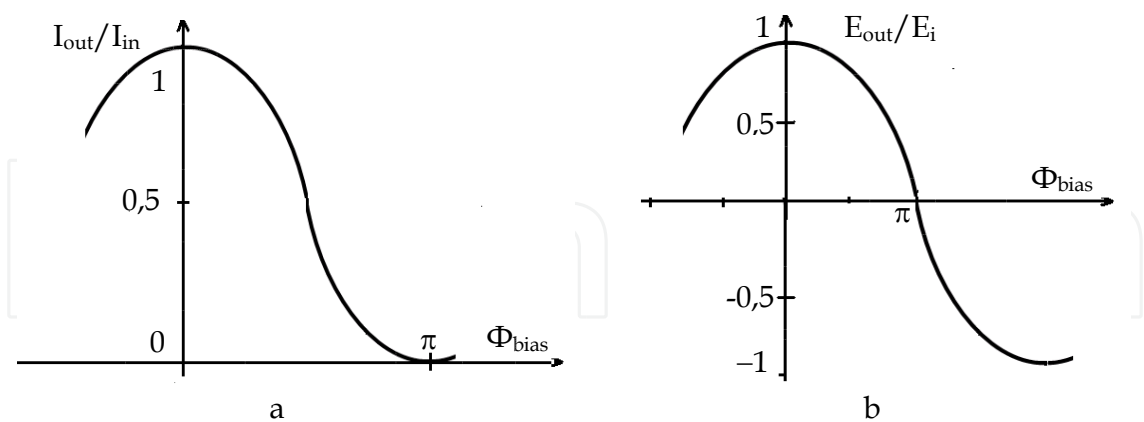
Fig. 10. MZM intensity (a) and electric field (b) modulation curve

This regime will also be available when $\Phi_{bias}=(2k-1)\pi$, however, the choice of k>1 does not satisfy the condition that the bias voltage should be of low amplitude otherwise the modulator's parameters undergo serious deviation, which will affect the spectrum conversion efficiency.

$$
\begin{aligned}
E_{out}(t) &= \left(E_0/\sqrt{2}\right)e^{j\omega t} \times \left[e^{jb\sin(\Omega t+\pi)} + e^{jb\sin(\Omega t)\,+\,j\Phi_{bias}} \right] = \\
&= \left(E_0/\sqrt{2}\right)e^{j\omega t} \times \left[2\sum_{n=1}^{\infty} J_{2n-1}(b)\left[e^{j(2n-1)\Omega t} - e^{-j(2n-1)\Omega t} \right] \right]
\end{aligned}
\tag{8}
$$

Analysis of (8) shows that the first term n=1 detects the presence in the spectrum of harmonics at frequency of $\omega_{+1}= \omega_0 + \Omega$ and $\omega_{-1} = \omega_0 - \Omega$, the second n=2 – the presence of harmonics at a frequency of $\omega_{+3} = \omega_0 + 3\Omega$ and $\omega_{-3} = \omega_0 - \Omega$, etc. So, the Il'in-Morozov method is realized.

The spectrum of the MZM output signal, when $\Phi_{bias}=\pi$, is multi-frequency and consists of two bands. They are located symmetrically around the suppressed carrier, the spectral components are at frequencies $\omega = \omega_0 \pm n\Omega$, where n = 1, 3, 5, ... Even harmonics are suppressed. The initial phases of the harmonics that make up the lower side band are π - radians different from the initial phases of the harmonics of the upper band.

The modulation index b has major influence on the spectral distribution of the output signal. This effect is examined further. Spectral distribution according to (8) is shown on fig. 11.

To obtain the two-frequency signal one should set the level of total harmonic distortion (THD) that is determined by the expression:

$$
THD = \sqrt{\left(E_3^2 + E_5^2\right)/E_1^2} .
\tag{9}
$$

Due to the smallness of the 7, 9, ...-orders harmonics' relative amplitudes their consideration is neglected. According to specified level of THD <1%, when the level of unwanted harmonics is negligible comparing to the amplitudes of the useful components, and the plot
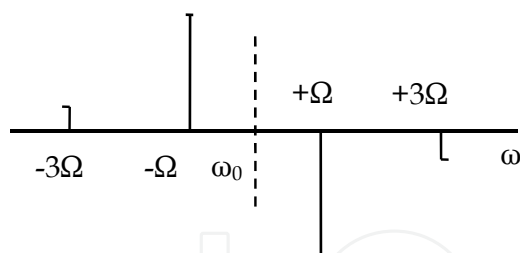
Fig. 11. Spectrum of (8)

of $J_n(b)$, we find that the fundamental condition for the two-frequency signal is b<0,49. Further increase of modulation index will lead to the fact that the relative amplitudes of 3rd and 5th orders harmonics will amount to the same order as the amplitude of spectral components of the 1st order. In particular the increase in the relative amplitudes of harmonics of third order leads to the fact, that for b = 3 the output signal will comprise four spectral lines.

5. Two-frequency reflectometry for FOS monitoring systems

Questions of OTFDR application efficiency for FOS monitoring on the examples of OTDR with two frequencies filling of probing pulse, non coherent OTFDR with LFM modulated components, and non coherent OTFDR for selective FOS probing are examined in this part.

5.1 OTDR with two frequencies filling of probing pulse

Structure of OTDR with two frequencies filling of probing pulse is synthesized on the basis of CO-OTDR (Jasenek, 2000). The main advantage of CO-OTDR is the opportunity of the maximal photo detector sensitivity maintenance which in an ideal case is determined by its quantum-mechanical limit $P_S / P_N = \eta P_0 / \hbar \omega \Delta F$. The basic destabilizing factors of CO-OTDR are instability of heterodyne frequency and default of polarizing conditions and spatial overlapping of measuring and basic beams at photo mixture. Undoubtedly, we can remove the mentioned above factors in fiber systems much easier, than in open, however methods used at it not always lead to desirable result.

In two-frequency OTDR system the frequency mode is realized inside a probing pulse with frequency components diversity on Ω. Ω is equal to tens or hundreds MHz and determines the central frequency of selective intermediate amplifier. Thus, measurements with carry of backscattering signal spectrum to area with a minimum level of photodetector noise are carried out.

Structure of OTDR with two frequencies filling of probing pulse is shown on fig. 12.

Optical radiation with angular frequency ω_0 divides on two parts in optical splitter OS1. Its one part is shifted on frequencies $\omega_0 \pm \Omega$ in TFLR forming electro optical modulator ((Il'in et al., 1997, O.G. Morozov & Sadeev, 2011) and received probing pulse with two frequencies filling incomes through OS2 into fiber under test. Backscattering radiation develops in OS3 with laser signal. Laser signal with power P_{LO} and backscattering signal with power $P_{RBS}(\omega_0 \pm \Omega)$ income on photodetector.

Application of methods and devices of symmetric two-frequency reflectometry in TFSC-OTDR allows to remove instability of frequency by application of two-frequency heterodyne
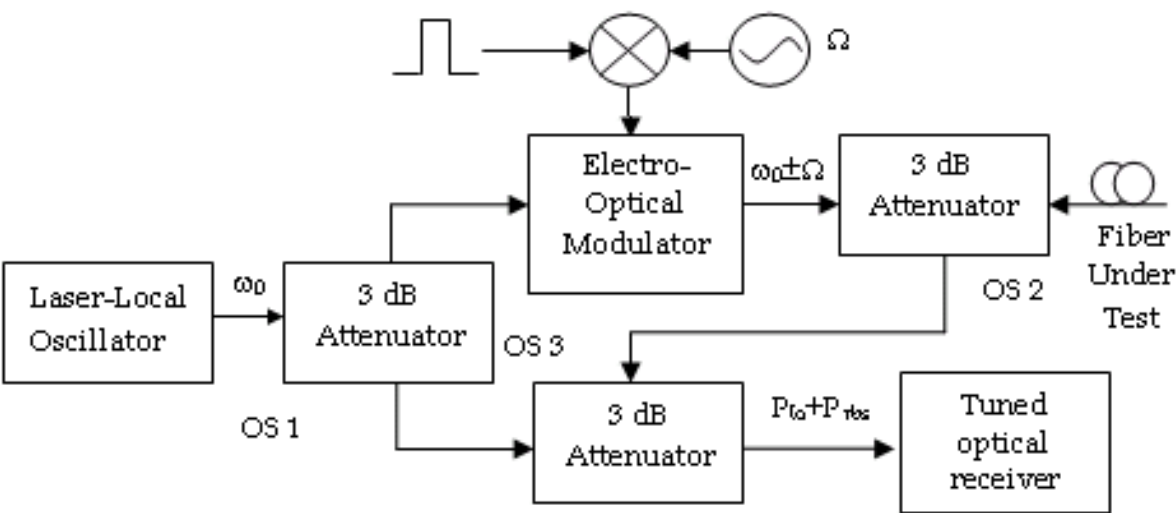
Fig. 12. Structure of OTDR with two frequencies filling of probing pulse

and also to provide performance of photo heterodyning conditions at direct two-frequency probing. In the second case for the signal/ noise ratio we shall receive

$$\frac{P_S}{P_N} = \frac{2P_1P_2(e\eta / \hbar\omega)^2}{2e\Delta F\left[i_\tau + P_{RBS}(e\eta / \hbar\omega)\right]} \approx \frac{P_1P_2(\eta / \hbar\omega)}{P_{RBS}\Delta F} . \tag{10}$$

The analysis of (10) at $P_{1,2} > P_{RBS}$ allows to approve, that, despite of reduction in sensitivity of the receiver in comparison with coherent reception, the bonus is received due to carry of an information signal spectrum to area with a minimum level of photo detector noise in comparison with direct detecting.

5.2 Non coherent OTFDR with LFM modulated components

Structure of non coherent OTFDR with LFM modulated TFSPR is synthesized on the basis of NC-OFDR (Abe et al., 1989, Froggatt, 1998, Pierce, 2000). We shall consider a piece of a fiber which is submitted on fig. 13. On a piece $0 < x < x_1$ there are the intrinsic losses α_1 caused by Raleigh scattering. On a piece $x_1 < x < x_2$ there are external losses caused by fiber microbends (defect, fig. 14). As at the appendix of mechanical tension ξ we receive decrease in a level of backscattering signal in comparison with a condition of rest, so losses in defect zone are equal $\alpha_2 = \alpha_i(1 - \Delta\alpha\xi)$, where α_i - initial losses caused by twisting. On a piece $x_2 < x < L$ with locked ends, where L – general length of a fiber, we come back to intrinsic losses α_1. Fibers remain permanently bent along their length after twisting. When the applied axial mechanical impact (e.g., stretching), the level of losses in the sensor becomes lower, as the curvature decreases. The relationship between optical loss and mechanical stress was obtained theoretically in the form shown below. Fiber radius of curvature R after two optical fibers twisting is given by

$$R = 1 / (2\pi)^2 l; \quad l = [p^2 + (2\pi r)^2]^{1/2} \tag{11}$$

where p_t – a twist step, r - half of the distance between the centers of two fibers, as shown in fig. 14, and l - length of the fiber, attributable to step twist.

When mechanical stress is applied uniformly over the entire length of the sensor, step twist changes and takes the value

$$p = p_i(1 + \xi),$$ (12)

where p_i - the initial step of twisting, when the force is not applied. On the other hand, the distance r decreases as optical fibers, stretching, compressed, and their main shell deformed.
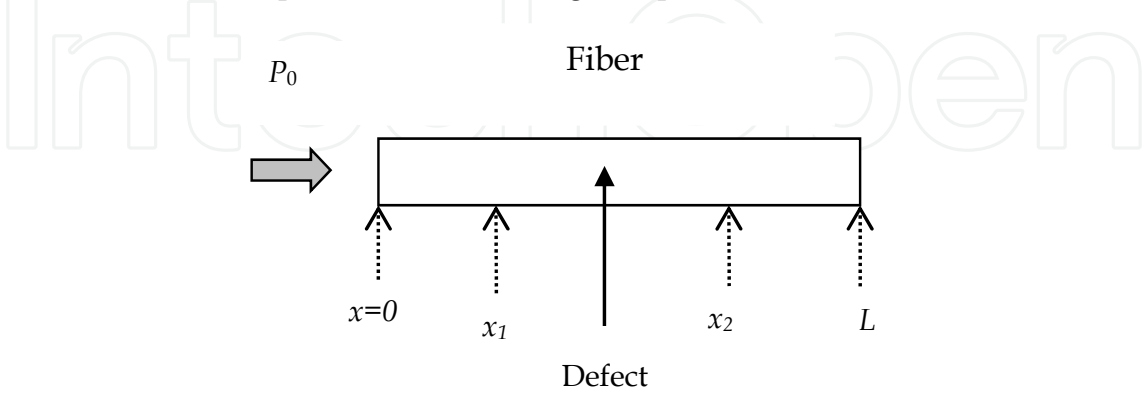

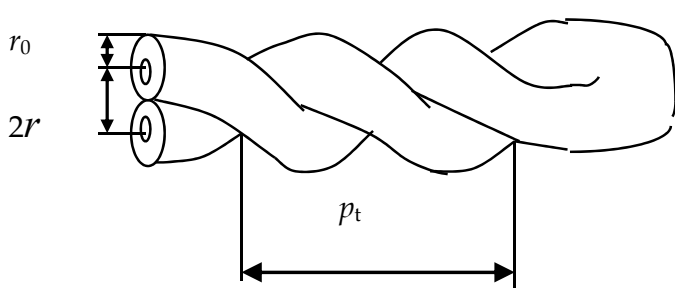Fig. 13. Structure of fiber under the test

Fig. 14. Structure of sensor part

We take into account closure of all FOS on the two twisted OF, under the assumption that the untwisted fiber, connecting the ends of the sensor has its own losses $\alpha_1 << \alpha_i$, then

$$\alpha(\xi) = 2\alpha_i(1 - 2\Delta\alpha\xi).$$ (13)

In fact, (13) shows that ceteris paribus, $\xi << 1 / \Delta\alpha$, $\alpha_1 << \alpha_i$, FOS on two twisted fiber with locked ends provides two fold the gradient changes of losses under the same applied load than the FOS on a twisted fiber with unlocked ends. Fig. 15 shows the calculated characteristics of FOS for various tensions and cross-elasticity *k*.

5.3 Non coherent OTFDR for resonant FOS monitoring

One of the main TFSPR applications is defined by an opportunity of testing resonant FOS, for example FBG or IFP. To analyze interaction of two-frequency signal we use some abstract circuit with normalized amplitude and phase dependences from frequency corresponding to FBG. Generalized amplitude-frequency characteristic of that abstract circuit we can define as follows
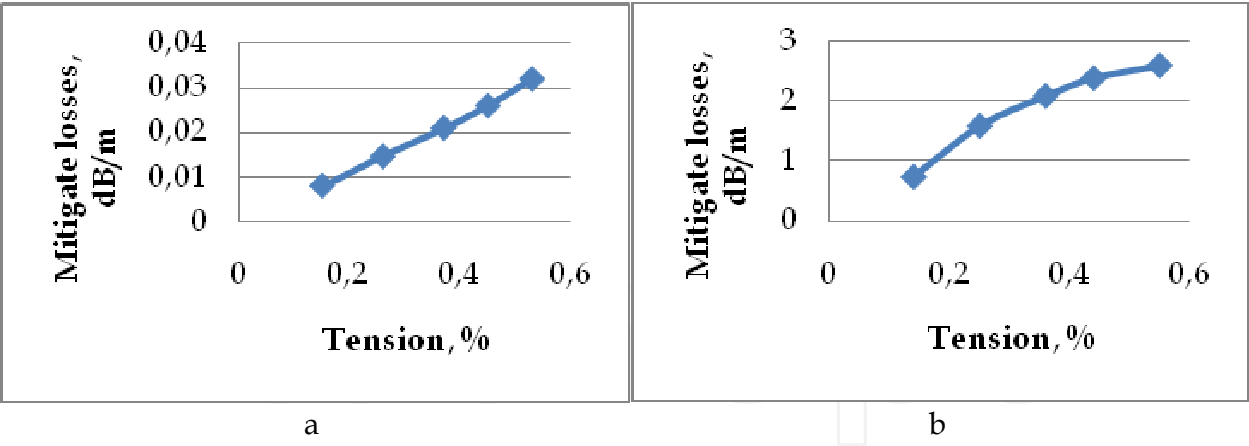
(k = 38 kg/mm² (a) and k = 1,2 kg/mm² (b))

Fig. 15. Characteristics of FOS on two twisted fiber with closed ends

$$Y(\varepsilon) = 1\Big/\sqrt{1 + \varepsilon_{0k}^2} \ . \tag{14}$$

Here $\varepsilon_{0k} = Q\big[(\omega/\omega_0) - (\omega_0/\omega)\big]$ is generalized circuit distortion.

Amplitude-frequency characteristic of circuit with two-frequency input signal is presented on fig. 16.

According to the average generalized signal distortion ε_0 the amplitude-frequency characteristic of abstract circuit could be divided on three parts:

1. if average generalized distortion lies in the interval $-\infty < \varepsilon_0 < -\varepsilon_0/2$ (I area), then; $\varepsilon_0 > \varepsilon_{02}$, $A_1/A_2 > 1$;
2. average generalized distortion lies in the interval $-\varepsilon_0/2 < \varepsilon_0 < \varepsilon_0/2$ (II area);
3. if average generalized distortion lies in the interval $-\varepsilon_0/2 < \varepsilon_0 < \infty$ (III area), then $\varepsilon_0 > \varepsilon_{02}$, $A_1/A_2 < 1$.

Taking into account that $\varepsilon_{01} = \varepsilon_0 + \Delta\varepsilon/2$ and $\varepsilon_{02} = \varepsilon_0 - \Delta\varepsilon/2$, we will get the equations for phase dependences of output two-frequency signal components on generalized distortion $\varphi_{1out}(\varepsilon_0)$ and $\varphi_{2out}(\varepsilon_0)$:

$$\varphi_{1out}(\varepsilon_0) = -arctg(\varepsilon_0 + \Delta\varepsilon/2), \tag{15}$$

$$\varphi_{2out}(\varepsilon_0) = -arctg(\varepsilon_0 - \Delta\varepsilon/2), \tag{16}$$

Amplitude and phase of two-frequency signal, as it follows from fig.16, depend on values of average generalized distortion ε_0 and frequency distortion $\Delta\varepsilon$.

Now we consider the changes of amplitude and phase of output two-frequency signal envelope $U_{output}(t)$ while it passes through the abstract circuit. Output two-frequency signal envelope is described as follows:

$$U_{output}(t) = E_{output}(t)cos(\omega_M t + \varphi_{output}(t)), \tag{17}$$

where $E_{output}(t)$ – resulting value of output two-frequency signal amplitude, $\varphi_{output}(t)$ – instantaneous phase, ω_M – instantaneous frequency of two-frequency signal.
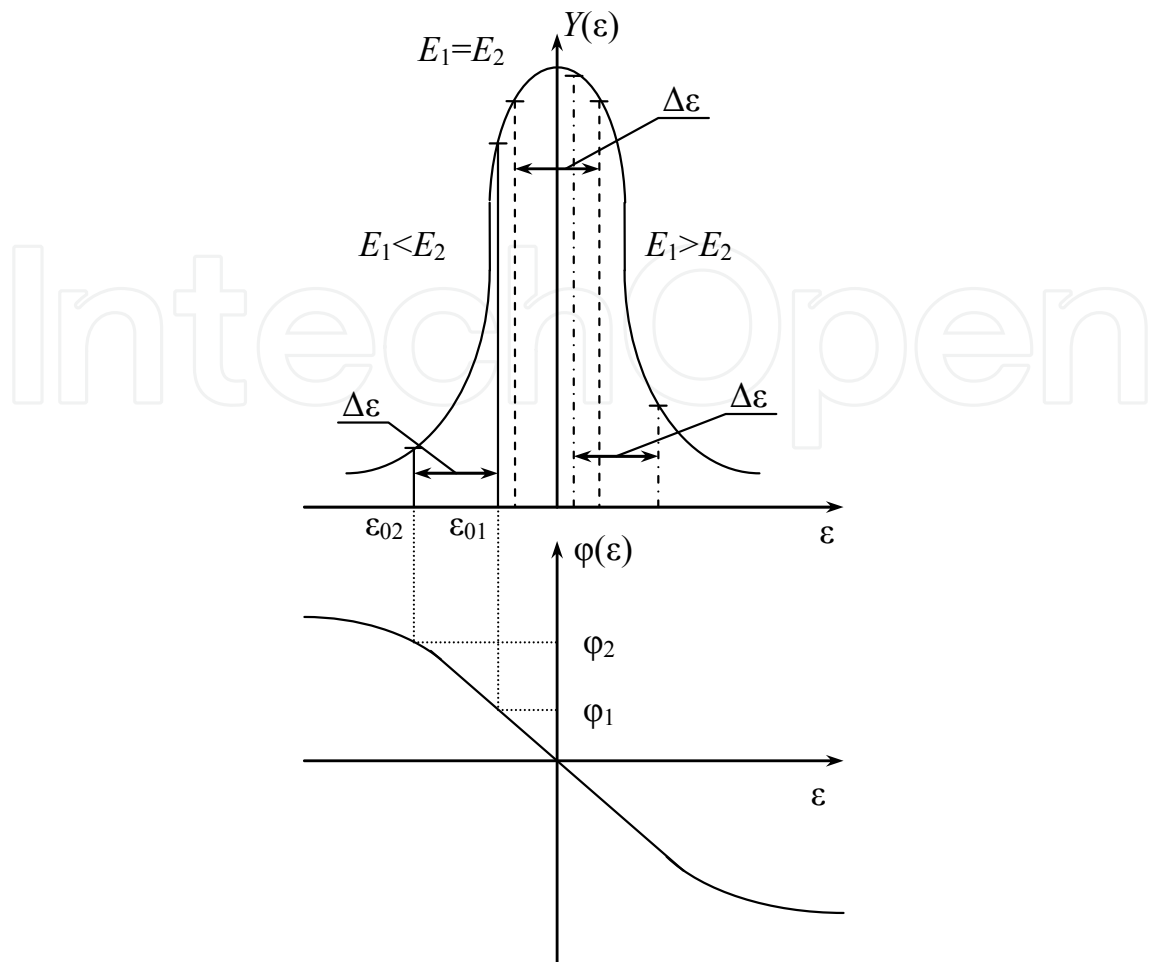
Fig. 16. Circuit amplitude-frequency characteristic with two-frequency input signal

Define the resulting value of two-frequency signal envelope amplitude E_{output} and then find the dependence of modulation index:

$$m = \sqrt{1+\left(\varepsilon_0 + \Delta\varepsilon / 2\right)^2} / \sqrt{1+\left(\varepsilon_0 - \Delta\varepsilon / 2\right)^2} . \qquad (18)$$

From this equation we see that modulation index depends on average generalized distortion on two-frequency signal ε_0 and on distortion between two-frequency signal components $\Delta\varepsilon$. Dependence of modulation index on average generalized distortion of two-frequency signal $m(\varepsilon_0)$ with different distortions between frequency components $\Delta\varepsilon$ is presented on fig. 17.

Fig. 17 shows that curve $m(\varepsilon_0)$ is continuous function, which achieve its maximum at $\varepsilon_0=0$. Function decreases to its minimum, then increases to unit value, and decreases again. Steepness of curve $m(\varepsilon_0)$ depends on frequency distortion $\Delta\varepsilon$. Let estimate that dependence.

Dependence of curve steepness $m(\varepsilon_0)$ on frequency distortion, $S(\Delta\varepsilon)$, is presented on fig. 18. Fig. 18 shows that this curve has maximum at $\Delta\varepsilon=2$, i.e. maximal curve steepness corresponds the case, when frequency distortion $\Delta\varepsilon$ is equal abstract circuit pass band. Consequently, when $\Delta\varepsilon=2$, estimation error of output signal envelope amplitude will be minor.
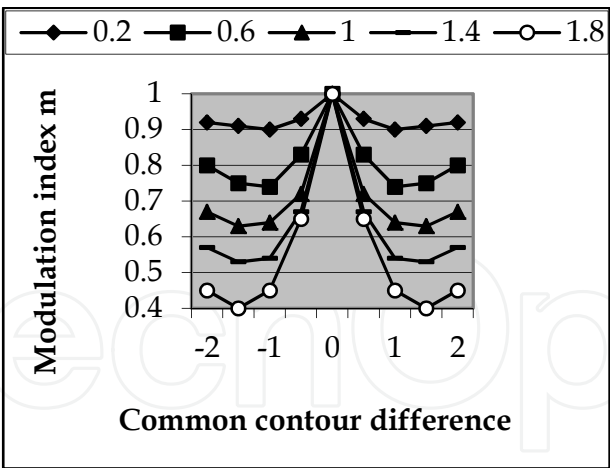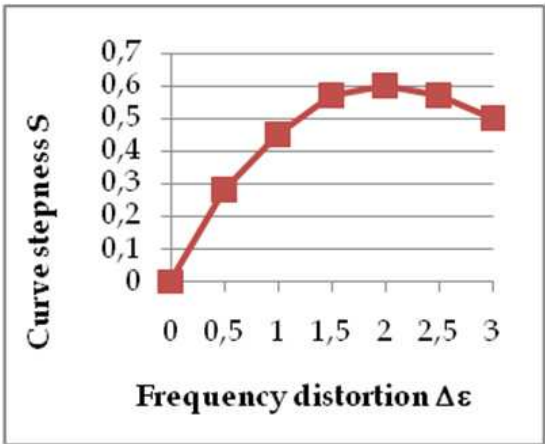
Fig. 17. Function m(ε_0)

Fig. 18. Function S($\Delta\varepsilon$)

Now consider dependence of phase shift of output signal components on average generalized signal distortion ε_0 with different values of distortion between frequencies $\Delta\varepsilon$. Calculation results are presented on fig. 19.
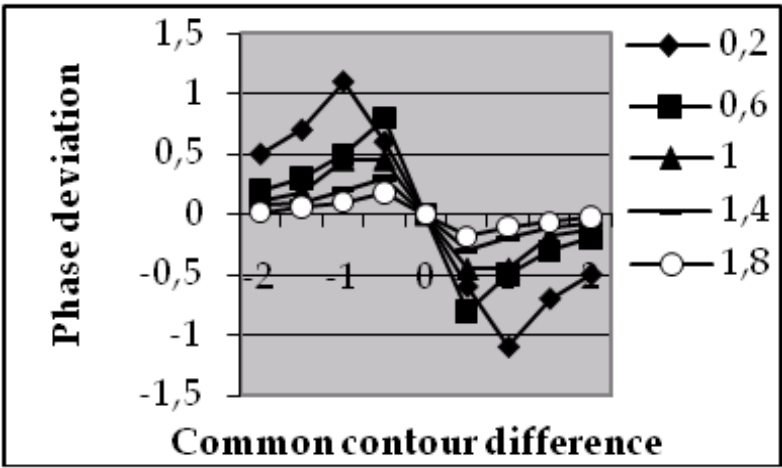

Fig. 19. Function $\Delta\varphi(\varepsilon_0)$

Fig. 19 shows that plot $\Delta\varphi(\varepsilon_0)$ is the third order curve which pass through zero when $\varepsilon_0=0$. Curve $\Delta\varphi(\varepsilon_0)$ is a continuous function which increases to maximum value, then decreases to minimum, and increases again.

Now we define the phase shift φ_{com} of output two-frequency signal envelope relatively input signal phase.

Phase shift of output signal envelope relatively input signal phase will consist:

$$\varphi_{com} = \varphi + \varphi_{1out}\left(-\infty < \varepsilon_0 < -\varepsilon_0/2 : \varepsilon_{01} > \varepsilon_{02}, E_1/E_2 > 1\right), \qquad (19)$$

$$\varphi_{com} = \varphi + \varphi_{2out}\left(+\infty < \varepsilon_0 < +\varepsilon_0/2 : \varepsilon_{01} > \varepsilon_{02}, E_1/E_2 < 1\right), \qquad (20)$$

where φ_{1out}, φ_{2out} – phase shifts of the first and the second output two-frequency signal components, φ – phase shift of resulting amplitude of output signal E_{output}.

After a series of complex transformations with notation of ε^+ and ε^- as $\varepsilon_0+\Delta\varepsilon/2$ and $\varepsilon_0-\Delta\varepsilon/2$ correspondingly we can rewrite equations (19) and (20) in a new way (upper index for ε^+ and lower – for ε^-):

$$\varphi_{com} = -\text{arctg}\left(\varepsilon^{\pm}\right) + \text{arctg}\left[\frac{\sin\left[-\text{arctg}\left(\varepsilon^{\mp}\right) + \text{arctg}\left(\varepsilon^{\pm}\right) + \Omega t\right]}{\left\{\left[1/\sqrt{1+(\varepsilon^+)^2}\right]/\left[1/\sqrt{1-(\varepsilon^-)^2}\right]\right\} + \cos\left[-\text{arctg}\left(\varepsilon^{\mp}\right) + \text{arctg}\left(\varepsilon^{\pm}\right) + \Omega t\right]}\right]. \quad (21)$$

From equation (21) we see that phase shift φ_{com} of output two-frequency signal envelope relatively input signal phase depends on value of average generalized signal distortion ε_0 and on value of frequency distortion $\Delta\varepsilon$. Calculation results of $\varphi_{com}(\varepsilon_0)$ for the case of $\varepsilon_{01} > \varepsilon_{02}$, $(E_{1out}/E_{2out})>1$ and different $\Delta\varepsilon$ are presented on fig. 20. Fig. 20 shows, that phase shift of output two-frequency signal envelope relatively phase of input signal will be equal to zero, when value of average generalized distortion $\varepsilon_0=0$.

Maximal sensitivity to average frequency of two-frequency signal change will be observed in case of equality of distortion between signal components $\Delta\varepsilon$ and pass band of abstract circuit.

Common equation for output two-frequency signal of abstract circuit for $-\infty < \varepsilon_0 < -\varepsilon_0/2$: $\varepsilon_{01} > \varepsilon_{02}, E_1/E_2>1$ is written as follows:

$$U_{output}(t) = \sqrt{E_{1out}^2 + E_{2out}^2 + 2E_{1out}E_{2out}\cos\left[\left(\varphi_{2out} - \varphi_{1out}\right) + \Omega t\right]} \cdot$$
$$\cdot\cos\left(\omega_M t + \left\{\varphi_1 + \arctan\left[\frac{\sin\left[\left(\varphi_{2out} - \varphi_{1out}\right) + \Omega t\right]}{E_{1out}/E_{2out} + \cos\left[\left(\varphi_{2out} - \varphi_{1out}\right) + \Omega t\right]}\right]\right\}\right) \cdot \qquad (22)$$

Calculation results of output signal envelope are shown on fig. 20-21. From fig. 20-21 we see, that at the same moment, when the average frequency of two-frequency signal achieve resonance frequency of abstract circuit, output signal envelope has the same phase as input two-frequency signal envelope. In this case modulation index of output two-frequency signal will be equal a unit value.
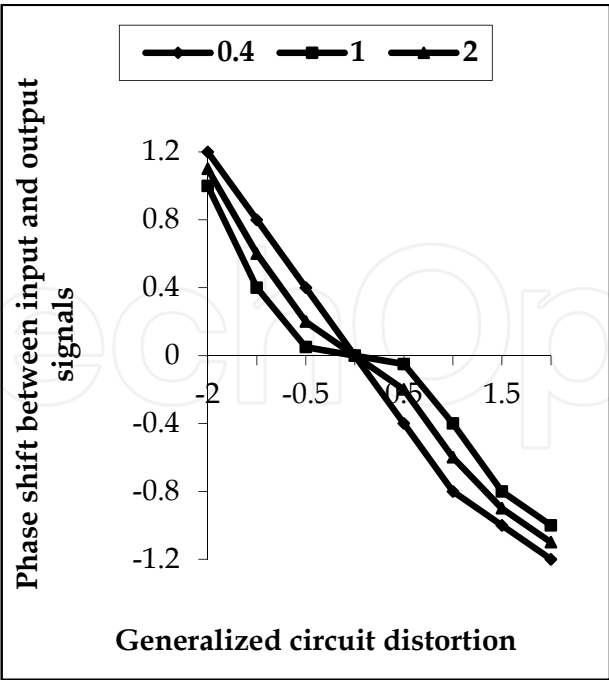
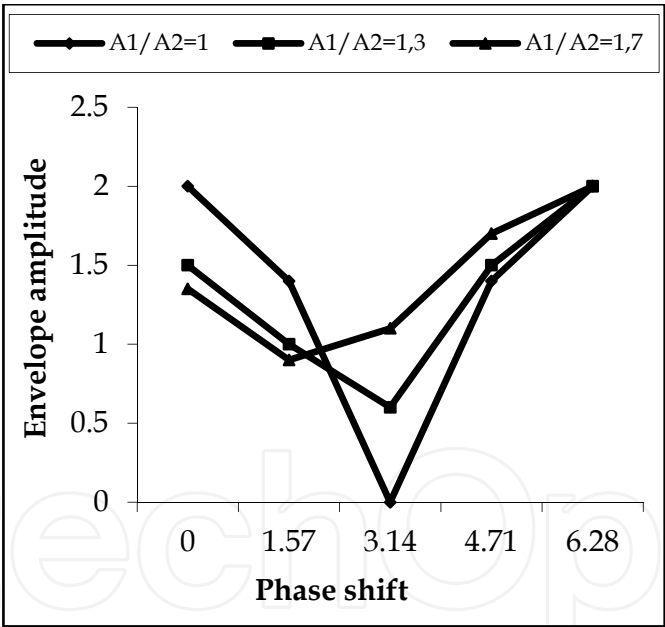Fig. 20. Dependence of $\Delta\varphi(\varepsilon_0)$ for different $\Delta\varepsilon$

Fig. 21. Two-frequency output signal envelope $U_{output}(\Omega t)$

In the research was considered the propagation of symmetrical two-frequency laser radiation through the widespread types of FBG. The following FBG types were considered: homogeneous FBG with high reflection index (the reflection spectrum contains intensive side lobes), FBG with Gaussian envelope of index profile (side lobes on the long-wave part of spectrum from the main peak are suppressed), FBG with phase π-shift (allow to form narrow band transmission areas), and chirped FBG (the resonance wavelength is changing along the grating in a specified way). This method also allows registering the FBG reflection spectrum displacement due the influence of temperature or strain.

6. OTFDR application for nonlinear effects measuring and compensation

6.1 Two-frequency detector of Brillouin scattering

Brillouin scattering carries vast amount of information about fiber conditions but has low energy level. That's why it's necessary to detect these types of scattering and determine their properties. Applying photomixing allows significantly increase the reflectometer systems sensitivity under the condition of weak signals and receives information from frequency pushing of backscattered signal spectrum. We offer to use two-frequency heterodyne (TFHet) and the second nonlinear receiver in the structure of Brillouin reflectometer (fig. 22).
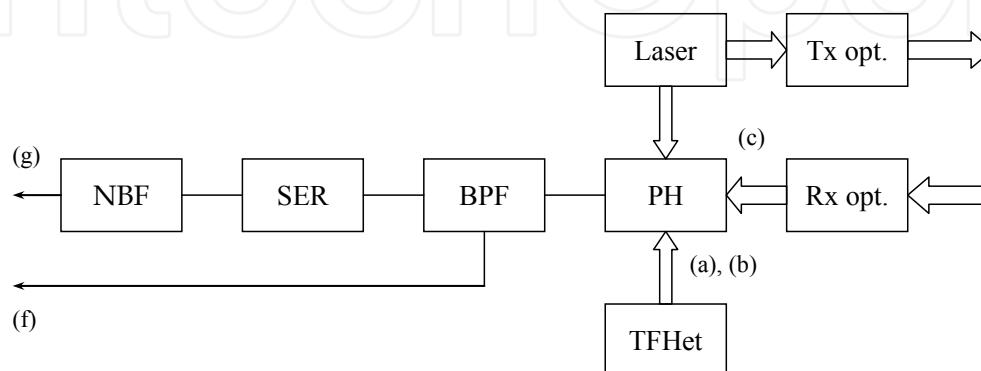
Fig. 22. Structure of two-frequency heterodyne system for OFS monitoring: NBF – narrow band filter, SER – square electronic receiver, BPF– band pass filter, PH – photo heterodyne, Rx opt – receiving optics, Tx opt – transmitting optics, TFHet – two-frequency heterodyne

Now we consider the signal passing through such system. Assuming that within photo detector aperture is provided the first order spatial error, amplitudes E_1 and E_2 of two-frequency signal components have the same polarization we can write the follow equation for electrical field intensity on receivers input:

$$E(t) = E_1 \cos(\omega_1 t + \varphi_1) + E_2 \cos(\omega_2 t + \varphi_2) + E_s \cos(\omega_s + \varphi_s), \qquad (23)$$

where ω_1, ω_2 and ω_s – angular frequencies of two-frequency signal components and receiving signal, φ_1, φ_2 and φ_s – its phases.

Taking into consideration Stoletov's rule, square characteristics of optical receivers and significant exceeding of heterodyne signal intensity above input signal we can say that output receiver signal consists on constant components and components with difference frequencies $(\omega_1–\omega_s)$, $(\omega_1–\omega_s)$ and $(\omega_1–\omega_2)$. Believing, that $A_1=A_2=A_h$, and the signal from photo detector output through blocking filter on frequency $\omega_1- \omega_2$ acts on the second square-law electronic receiver, we shall receive

$$I^2 \approx 4k^2 A_{bs}^2 A_h^2 \left\{ \begin{array}{l} 1 + \dfrac{1}{2}\cos 2(\omega_1 - \omega_{bs})t + \dfrac{1}{2}\cos 2(\omega_2 - \omega_{bs})t + \\ + \cos(\omega_1 + \omega_2 - 2\omega_{bs})t + \cos(\omega_1 - \omega_2)t \end{array} \right\}. \qquad (24)$$

If we install the narrow-band passing filter (NBF) on frequency $\omega_1–\omega_2$ on output of the second square-law electronic receiver (SER), its target signal will represent only change of amplitude of a backscattering Brillouin signal without taking into account frequencies

instability of the transmitter $I^2 \approx 4\beta^2 A_{bs}^2 A_h^2 \cos\Delta\omega_{bs}t$. The component with frequency $\omega_1 + \omega_2 - 2\omega_{bs}$ characterizes displacement of Brillouin signal frequency concerning frequencies ω_1 and ω_2, equal $\Delta\omega_{bs} = [(\omega_1 + \omega_2)/2] - \omega_{bs}$.

Thus, using of two-frequency heterodyne (TFHet) and second nonlinear electronic receiver (SER) allows to divide amplitude and frequency information channels, and also to generate the basic channel for elimination of frequency instability influence of the transmitter on the data of measurements. As a result of such modernization heterodyning system for OFS monitoring can be submitted as follows (fig. 22).

For confirmation of system serviceability its mathematical modeling (results put on fig. 23) and researches at the experimental stand has been carried out.
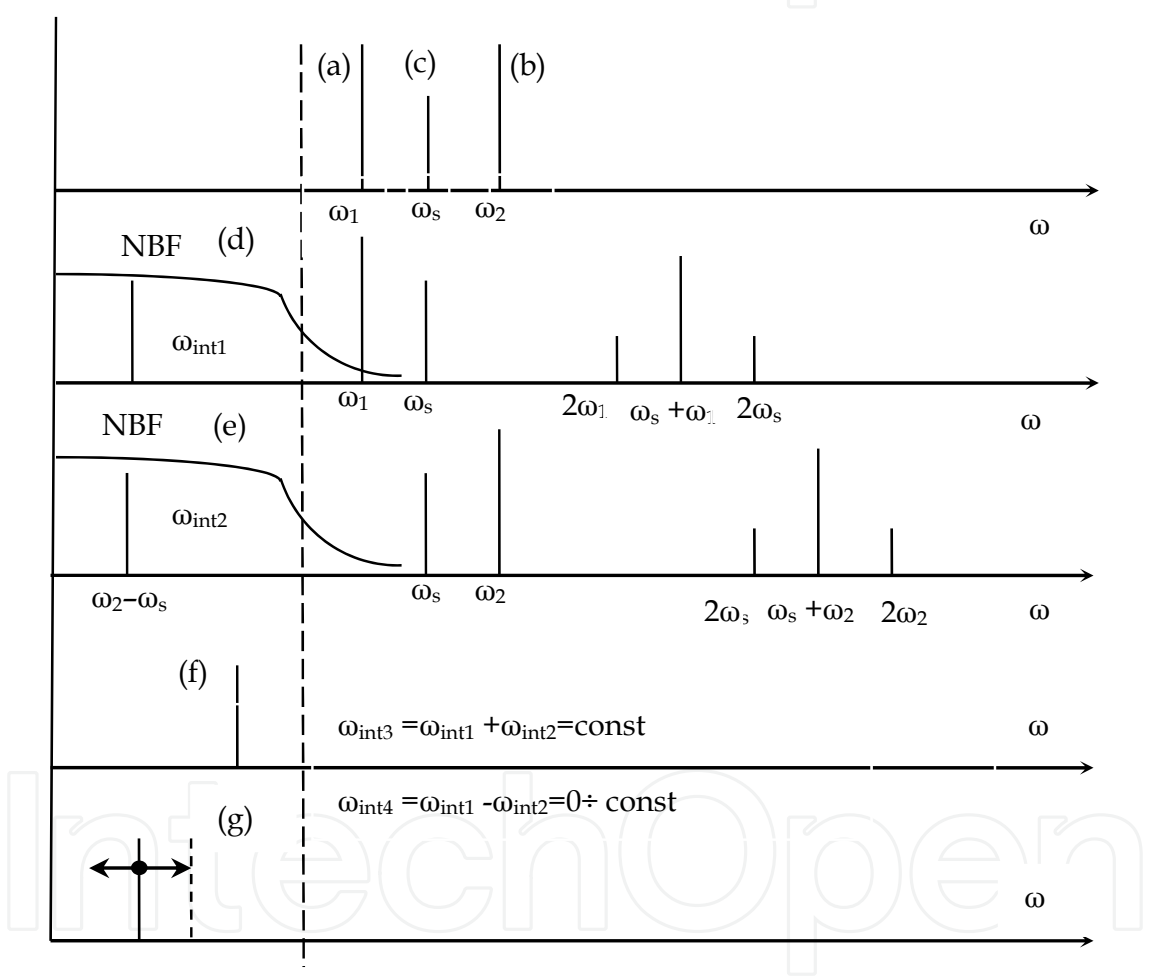
Fig. 23. Spectrograms in control points

The purpose of both researches was confirmation of opportunity to receive stable component on difference frequency and allocation of signal $\Delta\omega_{bs}$. Letters on fig. 22 designate control points, spectrograms in which are submitted on fig. 23. Experimentally received signals in the specified points are coincide with theoretic ones.

Thus, the opportunity of two-frequency heterodyne synthesis for OTFDR has been experimentally shown. It allows separately registering of useful signals of Brillouin scattering, as frequency information is separated from amplitude information. Using of two-frequency

heterodyne and second nonlinear electronic receiver allow to divide amplitude and frequency information channels, and also to generate the basic channel for elimination of frequency instability influence of the transmitter on the data of measurements. Applying OTFDR method for Brillouin scattering detecting doesn't need a series of measurements with retuning scanning frequency, as all information is receiving through one pass that significantly simplifies the measurement process in comparison with homodyne detection systems.

6.2 Double mode system for FWM reducing

Let's examine block of compensating signal source. It consists of light source and double mode radiation source (DMRS) as shown on Fig. 24a. In [2] detailed explanation of conversion method is given. According to this method we can get double mode radiation from single mode with known distribution of phases and amplitudes. Amplitudes of $\omega_0+\Omega=\omega_3$, $\omega_0-\Omega=\omega_1$ harmonics according to method are $E_n=\pi E_0/4$, where E_0 is amplitude of single mode radiation.

For polarization alignment of interacting signals quarter-wave plate can be used. According to this approach scheme shown on Fig. 24a undergoes some changes that are presented on Fig. 24b.
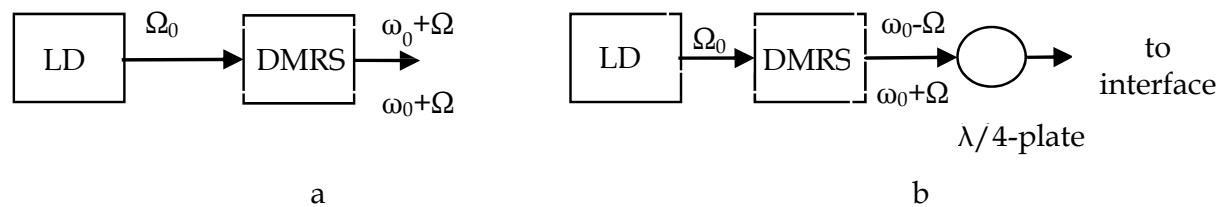

a
b

Fig. 24. Block-scheme of compensating signal source without (a) and with (b) polarization being taken in account

Selecting ω_0, Ω according to following well-known expressions with accordance to Fig.25a it's possible to suppress FWM – signal. Taking $\omega_0=\omega_2$, and Ω equal to interchannel interval for we reduce FWM harmonic that is located on ω_3, the same mechanism is applied for FWM – product reduction on ω_4, furthermore communication signals which are located on ω_1, ω_2 are amplified. Mechanism is briefly illustrated on Fig. 25,a and Fig. 25,b. As a variation of above described method another can be used in this case compensating signal comprises an amplitude modulated signal that is modulated according to expression below, such type signal's spectrum is illustrated on Fig. 26.

$$e(t) = E_0 \sin \omega_0 t[1 + m\cos(\Omega t + \pi)] = E_0 \sin \omega_0 t - \frac{mE_0}{2}\sin(\omega_0 t + \Omega + \pi) - \frac{mE_0}{2}\sin(\omega_0 t - \Omega - \pi) \quad (25)$$

As a result FWM signals on ω_3 and ω_4 are reduced from $A_{fwm.init}$ to A'_{fwm} and communication signals on ω_1 and ω_2 are amplified from $A_{sig.init}$ to A'_{sig} according to expression (26), (27), where m is modulation coefficient.

$$A'_{fwm} = A_{fwm.init} - mE_0/2 , \quad (26)$$

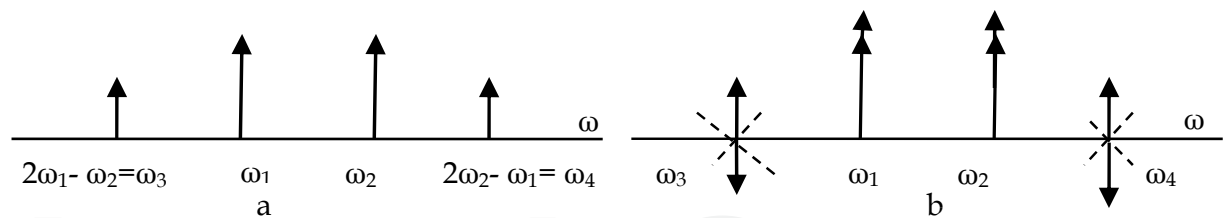$$A'_{sig} = A_{sig.init} - (mE_0/2) + E_0 . \quad (27)$$

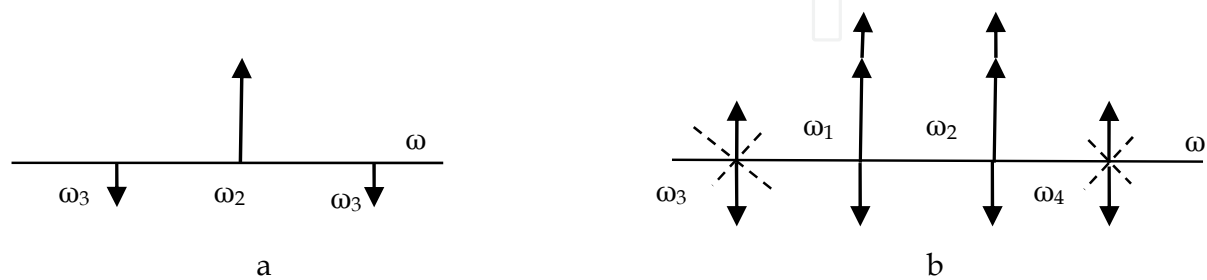Fig. 25. FWM (a) and interaction (b) between FWM, communication signal and double mode compensating signal

Fig. 26. AM-compensating signal (a) and interaction (b) between FWM, communication signal and AM-compensating signal.

For FWM products suppression it's claimed to use method based on conversion of single mode radiation into double that meets demands of amplitude, phase, and polarization alignment. This method is active i.e. communication channel that undergoes fading due to FWM is amplified, FWM products are suppressed to minimum levels also there is no need to use complex registration and measurement devices and components. In AM utilizing method it's necessary to select amplitudes of interacting signals carefully in order to prevent extra communication signal fading.

7. Miscellaneous applications

The miscellaneous application of OTFDR in bio sensing and TFSPR utilization in photonic microwave filter synthesis are mainly presented in (O.A. Stepustchenko et al., 2011) and (O.G. Morozov & Sadeev, 2011).

7.1 OTFDR in biosensors

Utilization of FBG with phase π-shift ROB assumes for measurement the central wavelength shift value of transmission Lorentz's contour with a half-width equal to pm units. For such values their estimation in terms of frequency is standard. Thus, the width of investigated contour spectrum is units of GHz. It is obvious, that application of broadband sources and optical spectrum analyzers for the decision of given problem is inefficient. High accuracy and resolution of measurements can reach at use of scanning Mickelson interferometer and the frequency-synchronized narrow-band laser sources. However maintenance of phase measurements stability in the first case and impossibility of high-speed feedback maintenance in the second do the decision very problematic as in case of static and dynamic measurements. The offered decision can be found at use of OTFDR. As we show in 5.3

OTFDR allows raising considerably power parities for modulation frequencies and to spend detecting on amplitude, phase and sign on a phase of differential frequency envelope with high stability of metrological characteristics.
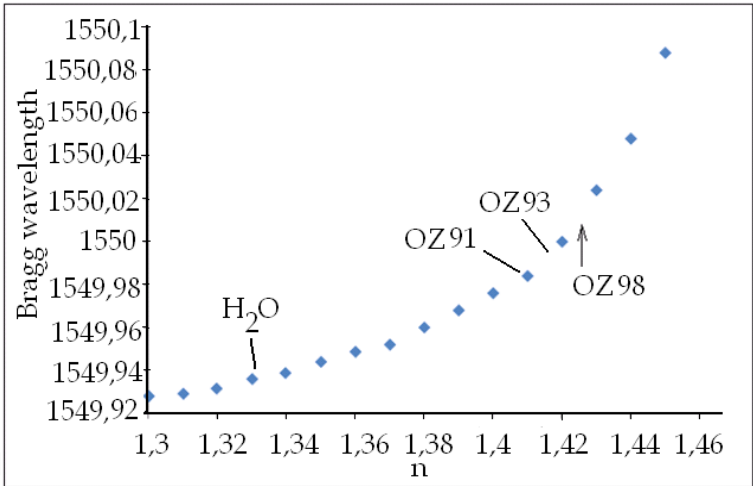

Fig. 27. The Bragg center wavelength as a function of the refractive factor of ambient material

Modeling results of biosensor in Optiwave Graiting software for red shifts of different materials concerning to water (n=1,33) are presented (fig. 27): gasoline with 91, 93, 98 octane numbers accordingly.

As comparison with results of another authors the dynamic range of wavelength shift is smaller, but enough to get sufficient resolution. From the other side experimental probing of this type ROB was realized by narrow band laser (kHz or MHz) with differential frequency in MHz range and its forming in Mach-Zehnder modulator. So SNR increase of measurements in 10-50 times were predicted. Experimental results was got on the base of SMF-28 Corning fibers.

7.2 All-optical microwave photonic filter based on two-frequency optical source

In this part we presented two tap photonic filter. Tunability is achieved by time delay adjusting which is performed by subcarriers separation. Proposed filter has the potential to implement several positive and negative components through bias voltage adjusting. First order notch located at 9 GHz might be tuned either by ω_0 or Ω adjusting.

To implement filter with two alternative coefficients we propose to utilize two-frequency radiation sources that was obtained by phase-amplitude modulation of initial single wavelength laser. The spectrum is shown on fig. 28,a, and spectrum after RF-modulation on fig. 28,b.

Overall filter frequency response H(f) is given on fig. 29.

To verify our mathematically based suggestions we have conducted simulation of filter in OptiSystem 7.0 simulation software tool and experimental base of Fiber Optic R&D Centre of our university. Firstly we obtained two separated wavelength by F GHz with the initial F/2 GHz signal. Then this signal was modulated in quadrature point in MZM by ω_{RF} – radio
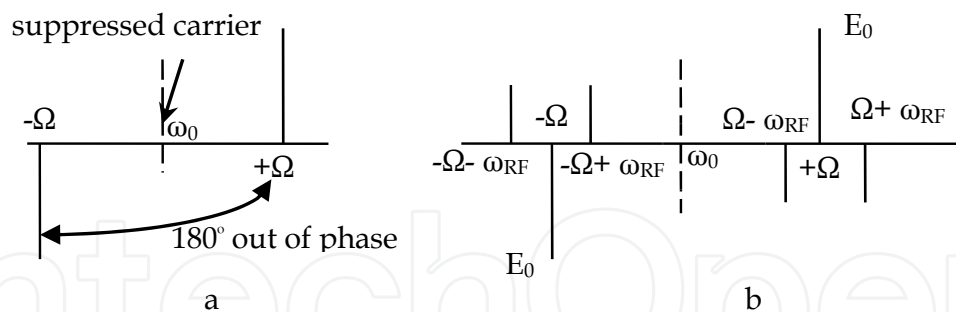
Fig. 28. Filter coefficients (a) and final spectrum of RF modulated signal
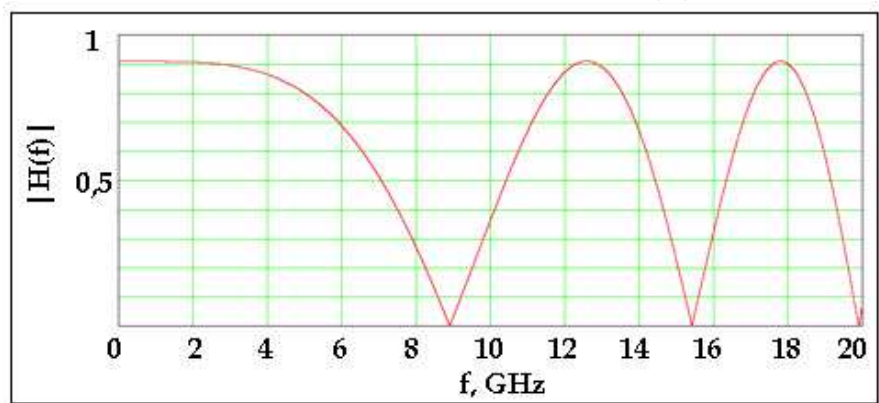

Fig. 29. Two tap filter frequency response *H(f)*

signal to be filtered. We used z=50 km of SMF fiber with D=16,5 ps/nm km dispersion thus achieving delay time T=ΔλLD. Frequency response was observed through RF spectrum analyzer tool and exactly matched FSR=1/T.

8. Conclusion

We reviewed the principle and the applications of the TFSPR technique. A variety of multiplexed sensing functions can be provided by the technique. As the examples, we introduced the systems of optical reflectometry, distributed lateral stress location sensors, multiplexed FBG and FFPI sensors. These systems possess the advantages of the continuous-wave operation, high resolution, high accuracy, and high speed. We have also developed a system to measure the strain distribution along an optical fiber through the Brillouin scattering. This system has already achieved 5-cm spatial resolution and 100 times higher dynamic range, respectively, than the conventional pulse-based time-domain techniques. Applications in the optical biosensing and microwave signal processing have also been demonstrated. System performance is being improved further with the perfection of two-frequency sources and application of four, six and etc. frequencies based on application of MZM comb-generators and elements of WDM technologies.

9. Acknowledgements

10. References

Abe, T., Mitsunaga, Y., Koga, H. (1989). A strain sensor using twisted optical fibers, *Journal of Lightwave Tech.*, Vol. 7, № 3, pp. 525-531.

Barnoski, M.K. & Jensen, S.M. (1976). Fiber waveguides a novel technique for investigating attenuation characteristics, *Applied Optics*, Vol. 15, N9, pp.212-216.

Gonorovskii, I. S. (1977). *Radio electronics circuits and signals*, Moscow, Russia.

Froggatt, M. & Moore, J. (1998). Distributed measurement of static strain in an optical fiber with multiple Bragg gratings at nominally equal wavelengths, *Applied Optics*, Vol. 37, pp.1741-1746.

Il'in, G.I. & Morozov, O.G. (1983). Method of one frequency coherent radiation convertion into two frequency, USSR patent N1338647, 20.04.2004.

Il'in, G.I. et al. (1995). LFM lidar with frequency conversion, *Atmospheric and Ocean Optics,* Vol. 8, N12, pp. 1871-1874.

Il'in, G.I. et al. (1996). Two-frequency oscillator for interferometers with polarization dived channels, In: *Optical Inspection and Micromeasurements*, edited by Christophe Gorecki, Proceedings of SPIE Vol. 2782 (SPIE, Bellingham, WA) pp. 814-819.

Jasenek, J. (2000). The theory and application of the fiber optic sensors with spread parameters, Slovak University of Technology in Bratislava, 2000, Available from http://www.eaeeie.org/theiere_bratislava/index.html.

Kharckevich, A.A. (1962). *Spectrums and signals*, Moscow, Russia.

Morozov, O.G. et al. (1999). Metrological features of laser interferometers with frequency conversion in supporting channel, In: *Optical Measurement Systems for Industrial Inspection*, edited by Malgorzata Kujawinska, Wolfgang Osten, Proceedings of SPIE Vol. 3824 (SPIE, Bellingham, WA) pp. 162-168.

Morozov, O.G. et al. (2006). Two-frequency analysis of fiber-optic structures, In: *Optical Technologies for Telecommunications 2005*, edited by V.A. Andreev, V.A. Burdin, A.H. Sultanov, Proceedings of SPIE Vol. 6277 (SPIE, Bellingham, WA) pp. 62770E.

Morozov, O.G. et al. (2008). Metrological aspects of symmetric double frequency and multi frequency reflectometry for fiber Bragg structures, In: *Optical Technologies for Telecommunications 2007*, edited by Vladimir A. Andreev, Vladimir A. Burdin, Oleg G. Morozov, Albert H. Sultanov, Proceedings of SPIE Vol. 7026 (SPIE, Bellingham, WA)pp. 70260J.

Morozov, O.G. et al. (2008). Methodology of symmetric double frequency reflectometry for selective fiber optic structures, In: *Optical Technologies for Telecommunications 2007*, edited by Vladimir A. Andreev, Vladimir A. Burdin, Oleg G. Morozov, Albert H. Sultanov, Proceedings of SPIE Vol. 7026 (SPIE, Bellingham, WA) pp. 70260I.

Morozov, O.G. et al. (2008). Double mode system for FWM reducing, In: *Optical Technologies for Telecommunications 2007*, edited by Vladimir A. Andreev, Vladimir A. Burdin, Oleg G. Morozov, Albert H. Sultanov, Proceedings of SPIE Vol. 7026 (SPIE, Bellingham, WA) pp. 702603.

Morozov, O.G. et al. (2009). All-optical microwave filter for ROF WDM systems based on double mode method, In: *Optical Technologies for Telecommunications 2008*, edited by Vladimir A. Andreev, Vladimir A. Burdin, Oleg G. Morozov, Albert H. Sultanov, Proceedings of SPIE Vol. 7374 (SPIE, Bellingham, WA) pp. 73740A.

Morozov, O.G. et al. (2010) Sensor on the twisted fibers for building construction monitoring, In: *Optical Technologies for Telecommunications 2009*, edited by Vladimir

A. Andreev, Vladimir A. Burdin, Oleg G. Morozov, Albert H. Sultanov, Proceedings of SPIE Vol. 7523 (SPIE, Bellingham, WA) pp. 75230J.

Morozov, G.A. et al. (2011). Structural minimization of fiber optic sensor nets for monitoring of dangerous materials storage, In: *Optical Technologies for Telecommunications 2010*, edited by Vladimir A. Andreev, Vladimir A. Burdin, Albert H. Sultanov, Oleg G. Morozov, Proceedings of SPIE Vol. 7992 (SPIE, Bellingham, WA) pp. 79920E.

Morozov, O.G. & Aibatov, D. L. (2007). Two-frequency scanning of FBG with arbitrary reflection spectrum, In: *Optical Technologies for Telecommunications 2006*, edited by Vladimir A. Andreev, Vladimir A. Burdin, Albert H. Sultanov, Proceedings of SPIE Vol. 6605 (SPIE, Bellingham, WA) pp. 660506.

Morozov, O.G. & Pol'ski, Y.E. (1996). Perspectives of fiber sensors based on optical reflectometry for nondestructive evaluation, In: *Nondestructive Evaluation of Materials and Composites*, edited by Steven R. Doctor, Carol A. Nove, George Y. Baaklini, Proceedings of SPIE Vol. 2944 (SPIE, Bellingham, WA) pp. 178-183.

Morozov, O.G. & Sadeev, T.S. (2011). All-optical microwave photonic filter based on two-frequency optical source, In: *Optical Technologies for Telecommunications 2010*, edited by Vladimir A. Andreev, Vladimir A. Burdin, Albert H. Sultanov, Oleg G. Morozov, Proceedings of SPIE Vol. 7992 (SPIE, Bellingham, WA) pp. 79920C.

Natanson, O.G. et al. (2005a). Development problems of frequency reflectometry for monitoring systems of optical fiber structures, In *Optical Technologies for Telecommunications*, edited by Vladimir A. Andreev, Vladimir A. Burdin, Albert H. Sultanov, Proceedings of SPIE Vol. 5854 (SPIE, Bellingham, WA) pp. 215-223.

Natanson, O.G. et al. (2005b). Reflectometry in open and fiber mediums: technology transfer, In: *Optical Technologies for Telecommunications*, edited by Vladimir A. Andreev, Vladimir A. Burdin, Albert H. Sultanov, Proceedings of SPIE Vol. 5854 (SPIE, Bellingham, WA) pp. 205-214.

Pierce, S.G. et al. Optical frequency domain reflectometry for microbend sensor demodulation", *Applied Optics*, Vol. 39, N25, pp.4569-4573.

Pol'ski, Y.E. & Morozov, O.G. (1998). Joint field of integrated fiber optic sensors for aircraft and spacecrafts safety parameters monitoring, In: *Nondestructive Evaluation of Aging Aircraft, Airports, and Aerospace Hardware II*, edited by Glenn A. Geithman, Gary E. Georgeson, Proceedings of SPIE Vol. 3397 (SPIE, Bellingham, WA) pp. 217-223.

Stepustchenko, O.A. et al. (2011). Optical refractometric FBG biosensors: problems of development and decision courses, In: *Optical Technologies for Telecommunications 2010*, edited by Vladimir A. Andreev, Vladimir A. Burdin, Albert H. Sultanov, Oleg G. Morozov, Proceedings of SPIE Vol. 7992 (SPIE, Bellingham, WA) pp. 79920D.

Zalyalov, R.G. et al. (1999). Optical frequency domain reflectometer for fiber structural testing, In: *Optical Measurement Systems for Industrial Inspection*, edited by Malgorzata Kujawinska, Wolfgang Osten, Proceedings of SPIE Vol. 3824 (SPIE, Bellingham, WA) pp. 274-279.
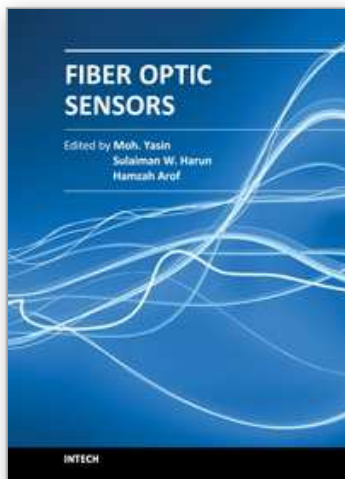
Fiber Optic Sensors

Edited by Dr Moh. Yasin

ISBN 978-953-307-922-6

Hard cover, 518 pages

Publisher InTech

Published online 22, February, 2012

Published in print edition February, 2012

This book presents a comprehensive account of recent advances and researches in fiber optic sensor technology. It consists of 21 chapters encompassing the recent progress in the subject, basic principles of various sensor types, their applications in structural health monitoring and the measurement of various physical, chemical and biological parameters. It also highlights the development of fiber optic sensors, their applications by providing various new methods for sensing and systems, and describing recent developments in fiber Bragg grating, tapered optical fiber, polymer optical fiber, long period fiber grating, reflectometry and interefometry based sensors. Edited by three scientists with a wide knowledge of the field and the community, the book brings together leading academics and practitioners in a comprehensive and incisive treatment of the subject. This is an essential reference for researchers working and teaching in optical fiber sensor technology, and for industrial users who need to be aware of current developments and new areas in optical fiber sensor devices.